Science of the Total Environment 642 (2018) 1008–1019

Contents lists available at ScienceDirect

Science of the Total Environment

journal homepage: www.elsevier.com/locate/scitotenv

Influence of pollutants on activity of aerosol cloud condensation nuclei (CCN) during pollution and post-rain periods in Guangzhou, southern China

Junyan Duan [a], Yanyu Wang [a], Xin Xie [a], Mei Li [b,*], Jun Tao [c], Yunfei Wu [d], Tiantao Cheng [a,e,**], Renjian Zhang [d], Yuehui Liu [a], Xiang Li [a], Qianshan He [f], Wei Gao [f], Jianpeng Wang [g,*]

[a] Shanghai Key Laboratory of Atmospheric Particle Pollution and Prevention (LAP^3), Department of Environmental Science and Engineering, Institute of Atmospheric Sciences, Fudan University, Shanghai 200433, China
[b] Institute of Mass Spectrometer and Atmospheric Environment, Jinan University, Guangzhou 510632, China
[c] South China Institute of Environmental Sciences, Ministry of Environmental Protection, Guangzhou 510655, China
[d] Key Laboratory of Region Climate-Environment Research for Temperate East Asia (TEA), Institute of Atmospheric Physics, Chinese Academy of Sciences, Beijing 100029, China
[e] Shanghai Institute of Eco-Chongming (SIEC), Shanghai 200062, China
[f] Shanghai Meteorological Bureau, Shanghai 20030, China
[g] Shanxi Meteorological Observatory, Xi'an 710014, China

HIGHLIGHTS

- Under different levels of pollutions, particle matter ($PM_{2.5}$) and number (CN) and CCN almost showed an opposite trend to aerosol activity (CCN/CN).
- Aerosol activity (CCN/CN) did not continue to rise with increasing soluble components and $PM_{2.5}$ levels.
- Different dominated heterogeneous reactions contributed to the changes of aerosol particles both in size and compositions directly modify the aerosol activity (CCN/CN).
- The hygroscopicity of particle was eventually modified by different PM formation mechanisms both in summer and winter.

GRAPHICAL ABSTRACT

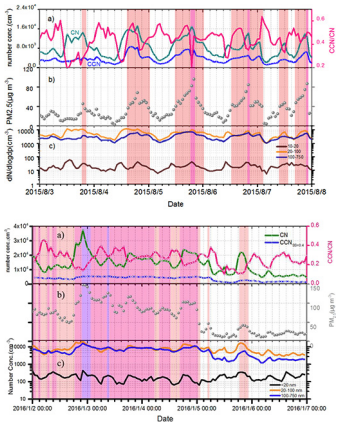

ARTICLE INFO

Article history:
Received 23 April 2018
Received in revised form 5 June 2018
Accepted 5 June 2018
Available online 19 June 2018

Editor: P. Kassomenos

ABSTRACT

Atmospheric pollutions have an important impact on aerosol, condensation nuclei (CN) and cloud condensation nuclei (CCN) loadings near the ground through disturbing particle size, number, chemical composition and reactions, mixing state, hygroscopicity, and so on. Aerosols and CCN were measured in urban Guangzhou during pollution and post-rain periods to examine effects of particulate pollutants on aerosol CCN activity and compare their mechanisms between summer and winter. In contrast with different levels of pollutions, particle matter ($PM_{2.5}$) and number (CN) and CCN almost showed an opposite trend to aerosol activity (CCN/CN). In summer, new particle formation (NPF) events triggered by photochemical reactions (e.g. O_3) always occurred in no-pollution daytime, and increased significantly CN and CCN as a dominant contributor to secondary aerosols.

* Corresponding authors.
** Correspondence to: T. Cheng, Shanghai Key Laboratory of Atmospheric Particle Pollution and Prevention (LAP^3), Department of Environmental Science and Engineering, Institute of Atmospheric Sciences, Fudan University, Shanghai 200433, China.
E-mail addresses: limei2007@163.com, (M. Li), ttcheng@fudan.edu.cn, (T. Cheng), xawjp@163.com (J. Wang).

https://doi.org/10.1016/j.scitotenv.2018.06.053
0048-9697/

Keywords:
Air pollution
Pollutant
Cloud condensation nuclei
Urban

Under pollution conditions, the gas-to-particle transition driven by photochemical reactions guided the formation and aging processes of particles in daytime, especially in changing soluble species, whereas atmospheric oxidation and heterogeneous reactions dominated at night. In winter, stagnant weather conditions, high pollutant levels and relatively high RH were in favor of particle growing and aging through enhancing secondary particle formation and heterogeneous reactions. The wet scavenging of precipitation reduced greatly CCN amount by scouring pre-existing particles in winter, and during post-rain period the photochemical reactions did not promote the burst of secondary particle formation in the absence of ozone, compared with summer. The results may provide insights into the relationship between aerosol moisture absorption and pollution that may be useful for improving air quality.

1. Introduction

Aerosol is an important component of the atmosphere that can affect the global climate system through direct and indirect effects, and impact air quality by reducing atmospheric visibility and forming pollution in the boundary layer (IPCC, 2013). Many studies have emphasized the significant role of cloud condensation nuclei (CCN) in cloud and precipitation (PR) formation, and have also stressed their sources, compositions, and evolutionary and scavenging processes (Yum et al., 2005; Rose et al., 2008; Andreae and Rosenfeld, 2008; Seinfeld and Pandis, 2006; Rosenfeld et al., 2008; Khain, 2009; Liu et al., 2011; Yuan et al., 2017).

In general, aerosols are emitted from primary sources and produced by secondary formation through transformation of precursor gases to solid particles (Fu and Chen, 2017). The physical and chemical properties of particles are the main factors to determine aerosol activation ability that vary widely in the atmosphere, such as particle size, chemical composition, and mixing state (Yum et al., 2005; Spracklen et al., 2008; Sihto et al., 2011; Matsui et al., 2011; Wex et al., 2010). Dusek et al. (2006) proposed that aerosol cloud-nucleating ability relies on particle size more so than on chemical composition. Kuwata et al. (2008) argued that considerable variation of CCN concentrations at lower supersaturation (SS) levels may be induced by changes in chemical composition. Wang et al. (2010) analyzed the importance of detailed information on the chemical composition and mixing state of aerosols for determining particle activation properties. In addition, the response of aerosol CCN activity to different particle mixing states implies a potential contribution of anthropogenic pollutants to CCN (Lance et al., 2013; Che et al., 2016). In particular, highly diverse organic and inorganic components complicate the micro-scale properties of aerosols, such as their structural functionality, hygroscopicity, solubility and volatility (Svensmark et al., 2017; Liu et al., 2014; Arndt et al., 2017). As particles age, ambient meteorological conditions can enhance their growth and eventually change their hygroscopicity (Crosbie et al., 2015; Mallet et al., 2017). For example, high relative humidity (RH) and low air convection velocity facilitate secondary aerosol formation and thus modify particle chemistry, especially under conditions of abundant gaseous pollutants (e.g. SO_2, NO_2 and NH_3) (Wu et al., 2015; Ding et al., 2013; Kristensen et al., 2016; Wang et al., 2016). Moreover, condensed vapors encountered during the particle growth process have an effect on particle surfactant properties, affecting volume during cloud-droplet formation and changing chemical composition to influence CCN properties (Ma et al., 2016). The Raoult and Kelvin effects are well-documented explanations of the possibility of activated aerosols (Rogers and Yau, 1989).

To date, field measurements have illustrated the important relationships among aerosol, CCN and pollution in areas such as Linan (Che et al., 2016), Beijing (Gunthe et al., 2011), Hong Kong (Meng et al., 2014), Seoul (Kim et al., 2017) and Jeju Island (Kuwata et al., 2008), Amazonia (Gunthe et al., 2009) and São Paulo (Almeida et al., 2014). The mutable properties of CCN can be modified by new particle formation (NPF), particle aging and growth, and pollutants encountered in various atmospheric environments (Kalkavouras et al., 2017; Kuang et al., 2009; Kalivitis et al., 2015; Gunthe et al., 2011; Dusek et al., 2006). Yue et al. (2010) found that the NPF events dominated by sulfate and organic material (OM) formation are important contributors to CCN budget. Wiedensohler et al. (2009) reported that growing nucleation-mode particles account for up to 80% of the total CCN concentration in Beijing, in contrast with the typical dominant accumulation mode. Anthropogenic emissions can elicit changes in particle chemical composition and size distribution, and at the same time increasing particle amounts aggravate the pollution situation (Kuwata and Kondo, 2008; Wang et al., 2010; Rose et al., 2010; Kerminen et al., 2012; Leng et al., 2014). Generally, pollution results in high loading of aerosol, which impacts CCN and thus cloud cover and PR over polluted areas (Zhao et al., 2006). Measurements collected on Tai mountain demonstrated the direct effect of regional pollution on the chemical species in cloud and fog droplets, and their altitudinal differences according to long-distance transport and local air masses (Wang et al., 2012). Rosenfeld et al. (2008) described an inverse relationship between air pollution and orographic PR, indicating that a greater abundance of submicron particles suppresses the PR-forming process by acting as cloud-drop condensation nuclei.

Guangzhou, a highly populated megacity located in the core of the Pearl River Delta (PRD) region in southern China, has experienced rapid economic development and industrialization for decades. This city is currently suffering from poor air quality due to abundant anthropogenic particles and gas pollutants (Peng et al., 2014; Lai et al., 2016; Tao et al., 2017; Zheng et al., 2012). Despite improved air quality in recent years, extreme pollution or hazy days still occur during all seasons (http://www.gdep.gov.cn/). Very few studies have reported the properties of CCN influenced by pollution in southern China.

In this study, we investigated aerosols and CCN in Guangzhou during pollution and after-rain periods both in summer and winter, for the purpose of understanding how pollutants age and affect aerosol CCN activities under different atmospheric conditions, and summarizing their possible parallel transfer mechanisms. Recent studies about Chinese pollutions had revealed and come out the conclusion that the reconsideration should be taken for changes of pollution situation. Viewed solely in terms of pollutants rather than weather, our results provide insights into the relationship between aerosols and pollution that may be useful for controlling pollution.

2. Instruments and data

2.1. Observation station

Field measurements were performed in July and August 2015, and in January 2016 in Guangzhou, China. The observation station was set on the roof of a building (about 50 m above ground level) at the South China Institute of Environmental Science (SCIES), Ministry of Environmental Protection (23.07°N, 113.21°E). Detailed information about this site was provided in our previous study (Duan et al., 2017).

2.2. Measurements

A CCN counter (CCN-100; DMT, USA) equipped with a continuous 500 cm^3/min flow stream and thermal gradient was employed to

measure CCN concentrations at five SS levels. Inside the counter, an optical particle counter (OPC) is utilized to detect activated droplets between 1 and 10 μm in size (Lance et al., 2006). The RH of inlet airflow was constrained to below 30% with a silica gel dryer. To maintain counting accuracy, the instrument was calibrated periodically for T gradient, flow, P, SS and OPC using standard ammonium sulfate according to the method of Rose et al. (2008). In addition, a zero determination was performed before and after every observation to diminish mechanical error. During the campaign, the observation interval was 10 min for each SS level, with several minutes needed after switching SS to regain a stable state. Therefore, we omitted CCN data collected before achieving stable SS from further analysis.

The Scanning Mobility Particle Sizer (SMPS 3080; TSI, USA) and Aerodynamics Particle Sizer (APS) were combined to measure the particle size distribution in the range of 13 nm–20 μm. Aerosol Instrument Management (AIM) software was utilized to make multiple charge and diffusion corrections. Aerodynamic diameter and mobility diameter were converted based on an assumption of spherical particles (Duan et al., 2017). Prior to sampling, the instruments were calibrated carefully using standard polystyrene latex (PSL) spheres. Moreover, inflowing ambient air passed through a Nafion tube (inlet through a 0.071-cm impactor) before entering the instruments. Zero determination and regular maintenance were conducted periodically to ensure reliable data.

A semi-continuous In-situ Gas and Aerosol Composition monitor system (IGAC) (model S-611; Fortelice International Co., Ltd., Taiwan) was employed to measure major chemical species including inorganic ions (NO_3^-, SO_4^{2-}, Cl^-, Ca^{2+}, NH_4^+, K^+ and Na^+) and precursor gases (HNO_3, SO_2 and NH_3) with a temporal resolution of 1 h. Nitrogen oxide (NO_x), sulfate dioxide (SO_2), carbon monoxide (CO) and ozone (O_3) were measured using gas analyzers with a 5-min resolution (Models 42i, 43i, 48i and 49i; Thermo Fisher Scientific Inc., USA). $PM_{2.5}$ mass concentration was determined using a tapered element oscillating microbalance (model 1400a; Rupprecht & Patashnick Co., Inc., USA). To avoid discrepancies caused by sea salt and nitrate in different seasons (Tao et al., 2012), a PM_{10} inlet (URG-2000-30DBQ; URG) and a $PM_{2.5}$ cyclone (sharp-cut cyclone; R&P) were employed in front of the sampling entrance during summer and winter, respectively.

Meteorological parameters, such as RH, T, WS, wind direction (WD), P and PR were measured with an automatic weather monitoring system (MAWS201; Vaisala Company, Finland). Atmospheric visibility (Vis.) data were collected online from the Weather Forecast & Reports site of TWC Product and Technology, LLC (https://www.wunderground.com).

2.3. Methodology

Air quality observations were divided into four levels based on the particulate pollutant mass concentrations (e.g. $PM_{2.5}$) according to the Chinese national ambient air quality standards (NAAQS). Hourly $PM_{2.5}$ levels exceeding 35 μg m^{-3} (Grade I), 75 μg m^{-3} (Grade II) and 125 μg m^{-3} (Grade III) were defined as light, moderate and heavy pollution conditions. When the pollution conditions persisted for over 4 h in 1 day, that day was considered a pollution day. High O_3 significantly contributes to aerosol formation and aging through photochemical or oxidation reactions, especially in summer, exerting a strong effect of solar radiation on aerosol evolution.

Deliquescence relative humidity (DRH) is a threshold for determining whether pre-existing hygroscopic particles can transfer from solid to liquid phase. DRH is sensitive to changes in ambient T and chemical species composition (Wang et al., 2016). If ambient RH increases to larger than DRH, a solid-liquid phase transition usually occurs and facilitates heterogeneous chemical reactions.

$$\ln \mathrm{DRH} = -\frac{M m_s L_s}{1000RT} \quad (1)$$

where M is the molar mass of water, m_s is the molality of a saturated solution, and L_s is the latent heat of salt fusion. When considering the lower volatile of $(NH_4)_2SO_4$ than NH_4NO_3 and NH_4Cl (Hu et al., 2014), in this study, ammonium sulfate was considered the preferentially formed species in particles to determine DRH. Moreover, the parameter kappa (κ) was used to characterize the hygroscopicity of aerosol particles (Rose et al., 2010; Zhao et al., 2015).

$$\Delta\mathrm{CCN}\ (\mathrm{SS1}-\mathrm{SS2}) = \mathrm{N}(\mathrm{CCN}_{ss1}) - \mathrm{N}(\mathrm{CCN}_{ss2}) \quad (2)$$

The increment of CCN was chosen as an indicator to reflect the effects of inorganic and organic compositions on aerosol CCN activity to some extent, representing the difference of aerosol hygroscopic and hydrophilic components, respectively. A high increment means that the majority of particle volume is made up of organic compounds. Although organic species differ in physicochemical properties, as a whole their contribution to particle hygroscopicity is far lower than that of inorganic species, especially soluble salt.

3. Results and discussion

3.1. Aerosol CCN activity during pollution days in summer

3.1.1. Changes of aerosols and CCN

The summer study period was from 3 to 7 August 2015, during which meteorological conditions were relatively stable, with low WS (~2.5 m/s), and high T (>27 °C) and RH (<80%). Over this whole period, although hourly $PM_{2.5}$ concentrations varied between 13 and 96 μg m^{-3} and reached high values on numerous occasions (Fig. 1), the average value of 35 μg m^{-3} represented relatively good air quality. In contrast, the PM level was higher than its typical in Guangzhou, but considerably lower than that at approximately the same time in northern Chinese cities such as Beijing (Liu et al., 2013), Xi'an (Xu et al., 2016) and Suzhou (Tian et al., 2016).

Overall, aerosol particle concentrations were generally higher during pollution episodes and lower during non-pollution periods, and exhibited distinct inter- and intra-day variations (Fig. 1). Specifically, when $PM_{2.5}$ was high, CCN and particle size concentration (CN) were also often at elevated values, but the corresponding CN/CCN ratio was unpredictable. At higher SS levels (>0.4%), CCN concentrations varied from 1419–1798 cm^{-3} to 11,575–14,307 cm^{-3}, while at lower SS (≤0.4%), they exhibited a small growth from 645–1172 cm^{-3} to 4017–8621 cm^{-3}. A similar discrepancy in the response of CCNs to SS has been observed on Jeju Island, Korea (Kuwata et al., 2008). The most abundant chemical species in particles, SO_4^{2-}, NO_3^- and NH_4^+ averaged 9.48 (±3.29) μg m^{-3}, 4.84 (±2.42) μg m^{-3} and 2.85 (±1.85) μg m^{-3}, respectively, and reached maxima 2–3-fold higher than their averages (Fig. 2).

To focus on the pollution period, it was divided into three subepisodes: light pollution on 3 August, moderate pollution on 4 to 6 August, and mitigating pollution on 7 August (Fig. 1). On 3 August, particle number (CN) increased dramatically at 10:00 LT (about 4-fold) and reached a maximum around 12:00 LT, and subsequently remained high for more than 8 h, while CCN and $PM_{2.5}$ varied only slightly. Nucleation mode (<20 nm) and Aitken mode (20–100 nm) particles increased sharply at 10:00 LT and then remained high for several hours. In particular, Aitken particles continued to increase until night, while accumulation mode (100 nm–2 μm) particles showed little fluctuation. According to the banana-shaped appearance of particle size spectra (Fig. S1), NPF events were considered the dominant contributor to increased CN and CCN. The sudden rise of fine particles driven by NPFs can generate more particles those can be activated into CCNs in urban environments (Sihto et al., 2011; Peng et al., 2014; Wiedensohler et al., 2009). From morning until sunset, O_3 increased from 10 to 178 μg m^{-3}, while inorganic ions in particles varied little. The high O_3 level accompanying CN implies a strong

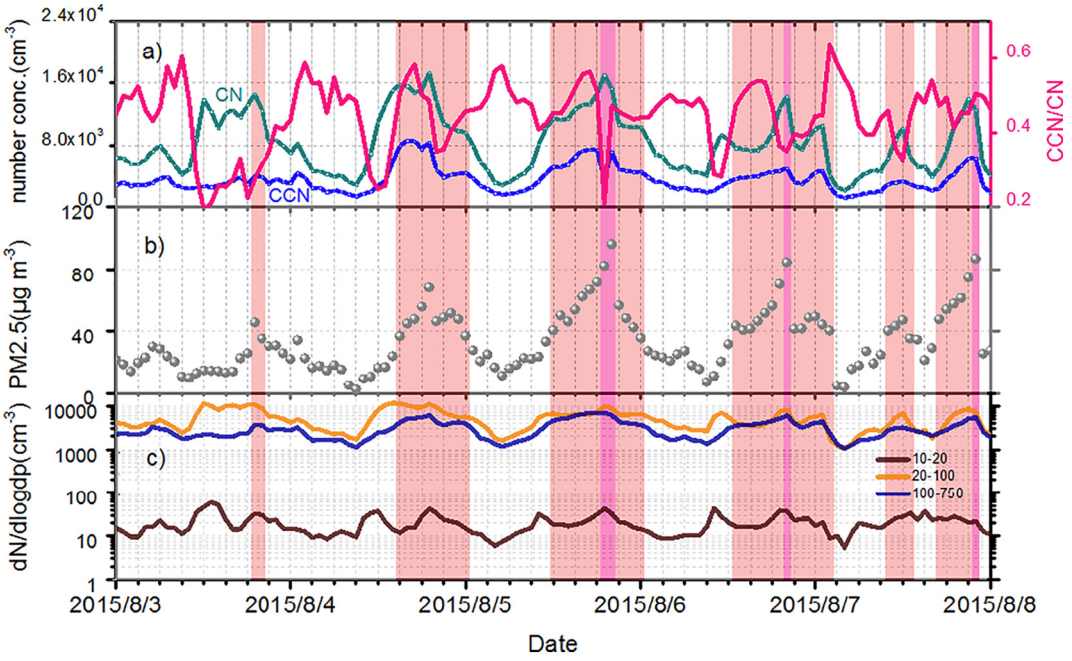

Fig. 1. Time series of hourly-averaged (a) CN, CCN and CCN/CN ratio, (b) $PM_{2.5}$ concentrations, and (c) 5-min mean particle number concentrations of nucleation, Aitken and accumulation modes from 3 to 7 August 2015. The background colors refer as to the periods of particulate pollution conditions, such as pink for light pollution, purple red for moderate pollution, and purple for heavy pollution.

effect of photochemistry on secondary aerosol formation through supply of OH and H_2O_2 radicals, especially after noon (Alfarra et al., 2012). Additionally, CCN/CN variation had basically a pattern opposite to CCN due to the extreme increase of CN at small sizes, which is not exhibited as CCN. We note that the highest $PM_{2.5}$ concentrations around 19:00 LT are partly attributable to vehicle emissions (He et al., 2008).

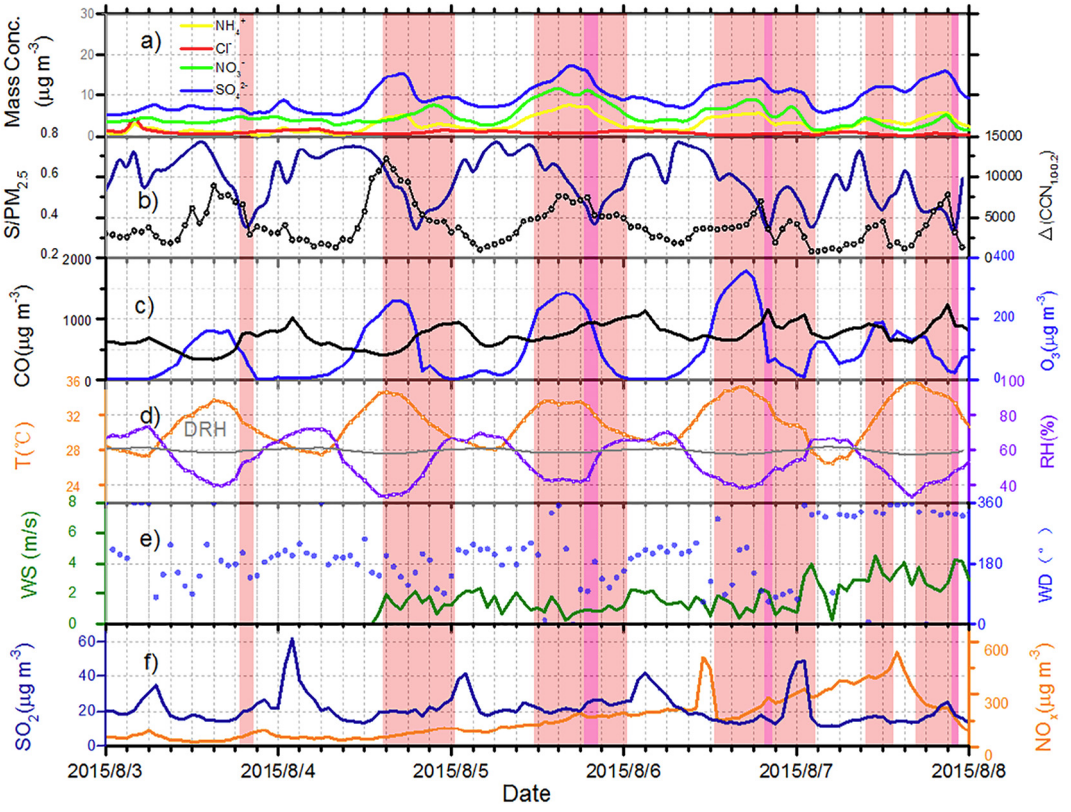

Fig. 2. Time series of hourly-averaged (a) major particle water-soluble inorganic ion concentrations, (b) soluble inorganic fraction of $PM_{2.5}$ ($S/PM_{2.5}$) and $\Delta CCN_{1.0-0.2}$ (increment of CCNs between SS = 1.0 and SS = 0.2), (c, f) gaseous species (CO, SO_2, NO_x, O_3), and (d, e) meteorology parameters of temperature (T), relative humidity (RH), wind direction (WD) and wind speed (WS) from 3 to 7 August 2015. The background colors are same with Fig. 1.

On 4 to 6 August, the pollution episodes were concentrated mainly in the afternoon and evening, lasting about 12 h from 12:00 LT to 24:00 LT. $PM_{2.5}$ and CN generally began to increase after 10:00 LT, and reached their maxima between 18:00 LT and 20:00 LT. During these pollution episodes, Aitken and accumulation particle concentrations were generally high, in particular, particle pooling was much greater than during no-pollution periods. Surprisingly, there seems to be a phase gap between PM level and particle activity: CCN/CN often peaked between 15:00 LT and 18:00 LT before $PM_{2.5}$ and CN, and the ratios fell to low values when their maxima approached. For instance, on 5 August, CN reached its highest level and CCN/CN dropped to its lowest at almost the same time (19:00 LT). As shown in Fig. 2, SO_4^{2-} and NH_4^+ increased after 10:00 LT and reached their maxima between 15:00 LT and 19:00 LT, similar to CCN/CN. SO_4^{2-} and NH_4^+ varied almost synchronously, whereas NO_3^- did not exactly imitate them, particularly on 4 August, when it increased continuously after 10:00 LT and reached its maximum after 21:00 LT.

3.1.2. Water-soluble chemical species of particles

Rose et al. (2010) explained the significant influence of chemical composition on aerosol CCN activity via absorption of water vapor. Although water-soluble chemical species are theoretically important for particle activation, they exhibit high temporal and spatial variability caused by many factors, such as emissions, secondary aerosol formation, particle aging and mixing (Wu et al., 2015; R.J. Huang et al., 2014; Asmi et al., 2011; Spracklen et al., 2008; Peng et al., 2014; Pierce and Adams, 2009). Pollution is viewed as an important factor via which aerosols change the water-soluble species of particles by triggering chemical reactions (e.g., photochemical, homogeneous, and heterogeneous reactions) due to abundant gaseous and solid pollutants (Kuwata et al., 2008; Wildt et al., 2014; Che et al., 2016; Ma et al., 2016). Moreover, in urban environments, the competition for condensable gases between pre-existing particles and newly formed particles associated with NPF suppresses the increase of particle size and hygroscopicity (Matsui et al., 2011).

Fig. 3 shows the statistical characteristics of water-soluble chemical species in particles by the levels of particulate pollutants. In general, greater particle mass ($PM_{2.5}$) was associated with higher particle number concentrations (CN, CCN) and higher soluble component contents (e.g. SO_4^{2-}). However, unlike the variables discussed above, aerosol activity (CCN/CN) did not continue to rise with increasing soluble components. Particles at the light pollution level were more activated than those measured under moderate pollution and relatively clean conditions. In addition, RH seems to be an important factor driving changes in water-soluble components and aerosol CCN activity. For example, at moderate pollution levels, RH may promote the formation of water-

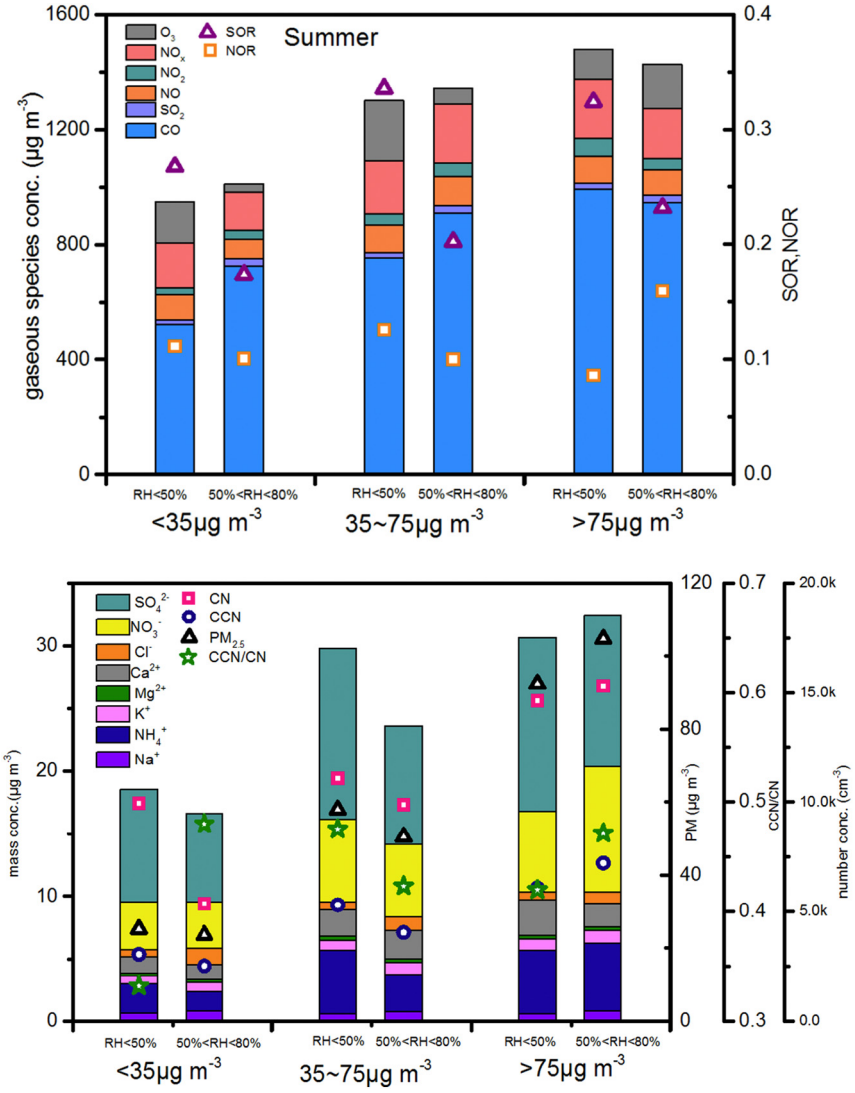

Fig. 3. Statistical characteristics of hourly gaseous species, SOR and NOR, particle water-soluble inorganic ions, and $PM_{2.5}$, CN and CCN at different levels of particulate pollutions for 3 to 7 August.

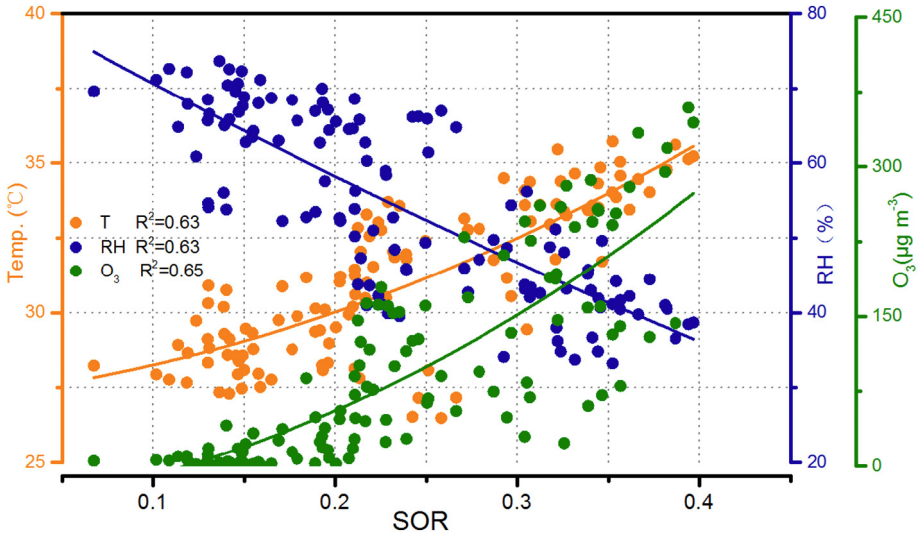

Fig. 4. Scatter plots of the transition ratios of SO_2 to SO_4^{2-} (SOR) vs. temperature, relative humidity (RH) and ozone concentration during 3 to 7 August.

soluble components and thus cause higher aerosol CCN activity, in particular of relatively high nitrogen oxidation ratio (NOR) due to greater nitrate formation enhanced by lower T and more moisture at night. During the relatively clear period from midnight to sunrise, with no obvious presence of anthropogenic emissions, the hygroscopicity of particles was mainly enhanced by liquid phase reactions. Sulfate transformation relies on gas and liquid phase transitions facilitated by solar radiation and stagnant meteorological conditions in summer (Grivas et al., 2012).

Sun et al. (2013) noted that gas particles participating in secondary formation are a major mechanism affecting PM evolution. Tian et al. (2016) proposed gas-phase oxidation by photochemical products (e.g. O_3) and heterogeneous oxidation as the two main methods by which trace gases are transferred onto particles. The increasing chemical fractions resulted in greater hygroscopicity and more particles activating into CCN, and therefore small particles with higher degree of oxidations had higher kappa values (Zhao et al., 2015). In addition, volatile organic compounds can always be transferred into secondary organic compounds (SOC) in particles through the photochemical effect (Alfarra et al., 2013). Kong et al. (2014) showed that nitrate participates in heterogeneous reactions with SO_2, accelerates the rate of sulfate formation, and leads to the formation of surface-adsorbed HNO_3 and gas-phase N_2O and HONO.

In Guangzhou, the fraction of aerosol organic compounds is higher than other cities in southern China due to the sources and quantity of anthropogenic pollutants (Tao et al., 2017). For particles smaller than 200 nm, chemical composition determines whether particles of a given size are able to activate as CCN, in particular the fraction of organic compounds. In Fig. 2b, the variation in ΔCCN between SS 1.0% and 0.2% is shown. Based on the response of CCN to different SS, a large increment represents a large fraction of insoluble compounds, especially organic matter. Because decreasing volatility and increasing hygroscopicity often covary with the increasing degree of oxidation, larger particles exhibit less size-dependence of composition than small particles (Vogel et al., 2016).

3.1.3. Influence of pollutants on aerosol CCN activity

All SO_4^{2-}, NO_3^- and NH_4^+ concentrations increased at the same pace as $PM_{2.5}$, but these values do not precisely represent the pollution state. The sulfur oxidation ratio (SOR) and NOR are used as indicators of the transition from SO_2 to SO_4^{2-} and NO_2 to NO_3^-, when sulfur and nitrate move between gaseous and particle phases (Leng et al., 2016). Fig. 4 shows the positive correlations of O_3 and T with SOR, whereas there is a negative correlation of RH with SOR, consistent with the results of Tian et al. (2016). The important effects of T on gas-phase oxidation, and of high RH on heterogeneous reactions, were described by Sun et al. (2014), including the Kelvin effect caused by differences in volatility that result in size-dependent composition due to partitioning of the gas-particle phase transition. Our field measurements revealed that pollutant formation was dominated by photochemical reactions, despite of the contribution of primary emissions. Although primary emissions affect both inorganic and organic fractions, SOC formation is an important factor to account for, especially during the photochemically active summer season. Due to a lack of organic data, the correlation coefficient modified by SO_4^{2-} can represent the organic fraction in particles, according to the method described by Grivas et al. (2012), and they found that the dominant pathway of SOC formation was a photochemical reaction closely related to oxidant levels, which intensified during the summer months, typically in the afternoon hours. Fig. 5 shows the strong relationship between $\Delta CCN_{1.0-0.2}$ and SO_4^{2-}. During the formation of pollutants, a large fraction of organic compounds leads to decreased hygroscopicity, in contrast to the pattern in inorganic compositions.

On the whole, photochemical reactions are the dominant method of pollution generation. For example, $\Delta CCN_{1.0-0.2}$ varied widely and reached its maximum during the CN burst on the mornings of 3 and 4

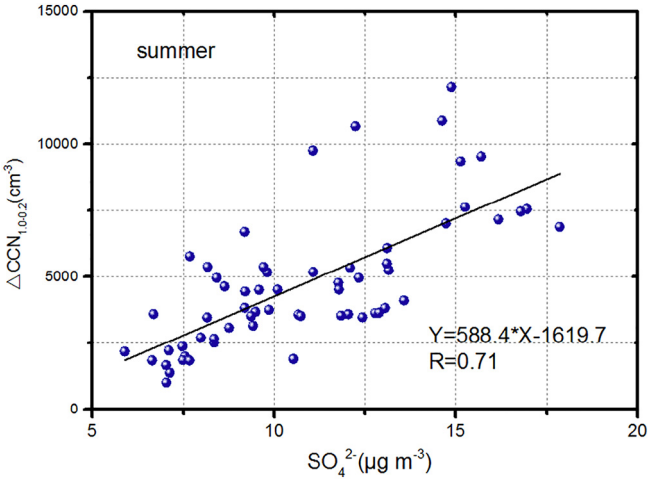

Fig. 5. $\Delta CCN_{1.0-0.2}$ as a function of SO_4^{2-} concentrations in polluted periods during 3 to 7 August (tagged by colors in Fig. 1).

August (Fig. 2b). Based on CCN properties, $\Delta CCN_{1.0-0.2}$ is typically sensitive to changes in the hydrophobic components (e.g., organic matter) of particulate matter. In terms of the hygroscopicity of particles, the corresponding kappa value remains low. The reason for this trend may be that newly formed particles are accompanied by organic compounds (Dai et al., 2017). During the period of strong solar radiation in the afternoon, although inorganic chemical components increased, their proportion in $PM_{2.5}$ ($S/PM_{2.5}$) gradually decreased, probably due to the generation of organic components via photochemical reactions.

Even when the effects of photochemical reactions are reduced at night, rapidly increasing NO_x expedite atmospheric oxidation to prompt particle formation and growth, which may be due to the transition toward more primary gas pollutants formed through heterogeneous reactions at night (Wang et al., 2016). Zhao et al. (2015) demonstrated that atmospheric aging leads to a change in aerosol mixing state, e.g., from an external mixture to one that is more internally mixed, possibly due to aqueous phase processing. Heterogeneous reactions and irreversible uptake of low-volatility compounds may also affect the size dependence of composition due to varying surface-to-volume ratio of particles of different sizes. In ambient atmosphere, the primary formation pathways include gas-phase photochemical production of HNO_3 during daytime and heterogeneous hydrolysis of N_2O_5 at nighttime. For example, on 4 August, the O_3 concentration reached its highest level of 260 μg m^{-3} at 16:00–17:00 LT and decreased until 20:00 LT, likely due to NO_2 depleting O_3 and producing NO_3 and/or N_2O_5, which readily form HNO_3 with H_2O. Facilitated by increasing RH, the continuous increase of nitrate was caused by neutralization in particles. Due to elevated anthropogenic emissions and no notable presence of O_3 after 21:00 LT, the major inorganic components increased gradually, but shifted from nitrate- to sulfate-dominant particles for stability. Nitrate is labile at high T, and can also be formed via NO_2 oxidation by OH radical and H_2O_2 (Cheng et al., 2016).

Previous studies have investigated the significant role of photochemical reactions in new and secondary particle formation. Ding et al. (2013) reported that high oxidant levels can lead to SO_2 transformation into sulfate and high rates of secondary aerosol formation under high-O_3 conditions. The remaining large fraction of NO_2 and O_3 drive atmospheric oxidation, leading to efficient PM mass and particle size growth (Wang et al., 2015). Also, as illustrated by Qi et al. (2015), high levels of $PM_{2.5}$ and large particle geometric mean diameter (GMD) retard NPF under high oxidization capacity conditions in summer, emphasizing the important role of secondary transformation. Nevertheless, it is feasible that worsening pollution may weaken the formation of new particles while promote particle growth and aging.

The single hygroscopicity parameter κ, and thus the CCN activity of secondary inorganic aerosol (SIA) particles, represent the total CCN population at all sizes. In Figs. 6 and 7, kappa and the inorganic chemical

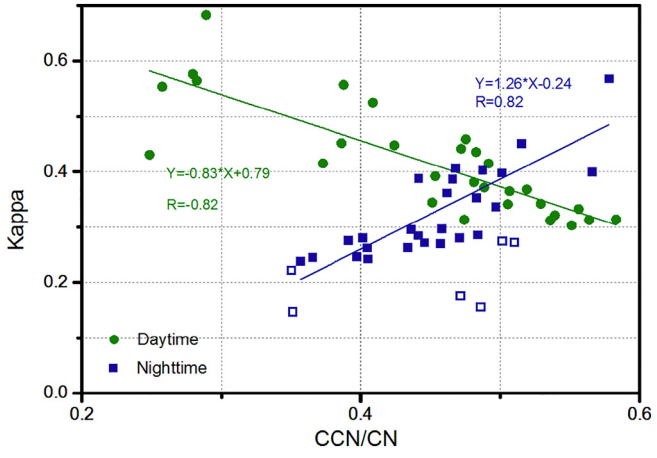

Fig. 6. Scatter plots of CCN/CN vs. particle hygroscopic parameter kappa (κ) in daytime and nighttime during 4 to 6 August.

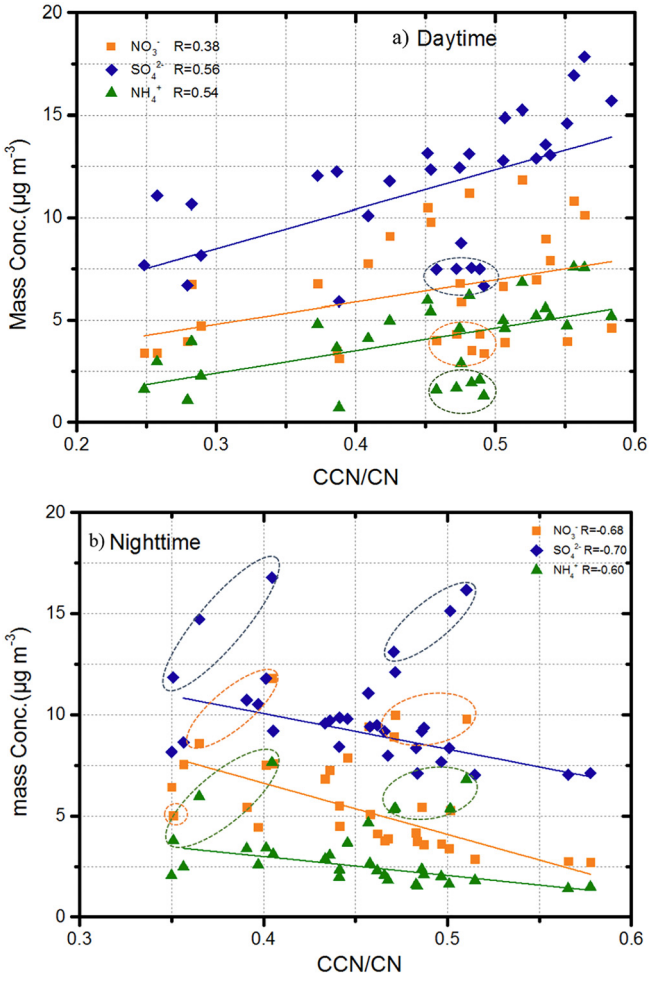

Fig. 7. Relationship between CCN/CN and major inorganic chemical compositions in (a) daytime and (b) nighttime of polluted days during 3 to 7 August.

composition of aerosols showed differing trends when viewed as functions of CCN/CN in daytime and nighttime. From the analysis above, it is evident that photochemical reactions can also promote the transformation of gaseous pollutants (e.g., NO_2, SO_2) and semi-volatile compounds into secondary aerosols and highly oxidized species, including organic components of particles. Despite heterogeneous reactions continuing to occur at night, the particle chemical component concentrations reduced. These pollution formation conditions allowed more detailed study of secondary organic formation process, which may influence CCN activity in summer. Additionally, to our knowledge, increasing T, rising planetary boundary layer, strong solar radiation and instable atmospheric convection also provide favorable conditions for accelerating the mixture and reaction of atmospheric species.

3.2. Aerosol CCN activity during pollution days in winter

3.2.1. Changes of aerosols and CCN

The study period in winter was 2 to 4 January 2016, including the New Year holiday on 2 to 3 January (Fig. 8). During this period, stable meteorological conditions were unfavorable for vertical and horizontal diffusion of pollutants, including high RH with low T and WS. Previous studies have found that a stagnant weather cycle facilitates regional pollution formation (e.g., haze) and causes heavy pollution periods to last longer in winter (Leng et al., 2014). Overall, hourly $PM_{2.5}$ concentrations were mostly higher than 75 μg m^{-3}, and sometimes exceeded 100 μg m^{-3}, with a maximum of 150 μg m^{-3} at midnight on 2 January. CN and $PM_{2.5}$ concentrations exhibited distinct inter- and intra-day

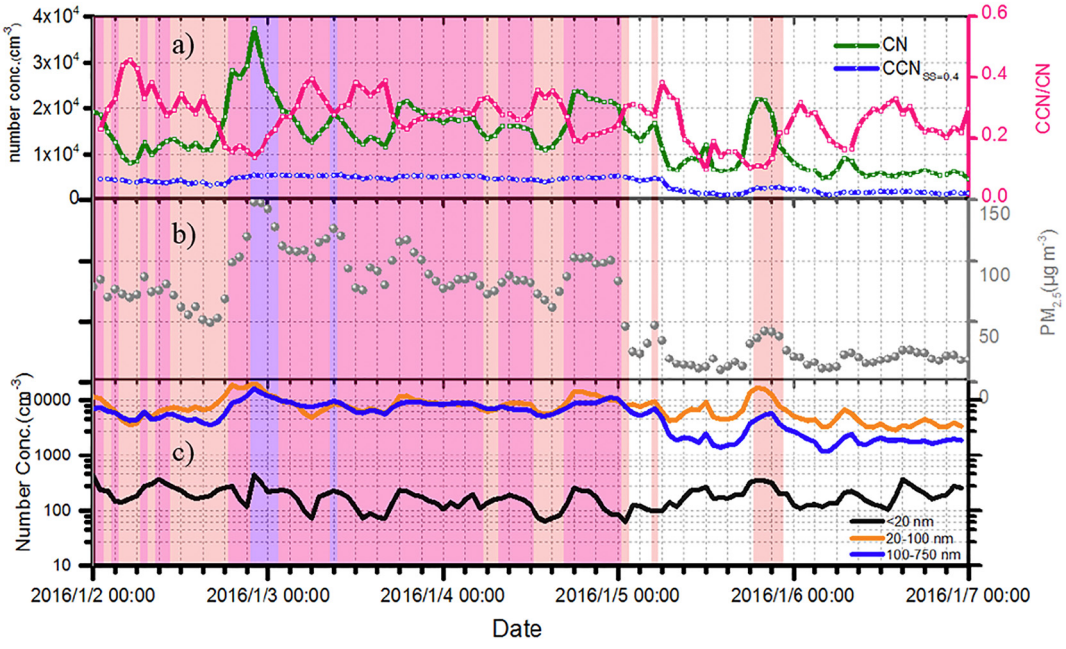

Fig. 8. Similar as Fig. 1, but for 2 to 7 January 2016.

variations, while variation in CCN was not obvious. When $PM_{2.5}$ and CN had high values, the corresponding CN/CCN ratio was low. CN and CCN maintained higher levels than in summer, with averages of 20,000 cm^{-3} and 5000 cm^{-3}, respectively. The abundances of chemical species in particles, SO_4^{2-}, NO_3^- and NH_4^+, averaged 13.66 (±7.12) μg m^{-3}, 20.73 (±15.36) μg m^{-3}, and 11.38 (±7.25) μg m^{-3}, respectively, and reached maxima higher than their averages by 2–3-fold (Fig. 9a).

On 2 January, $PM_{2.5}$ began to rise at 16:00 LT and reached its maximum of 150 μg m^{-3} between 21:00 LT and 24:00 LT. CN also increased sharply after 16:00 LT and reached a peak (38,000 cm^{-3}) at around 22:00 LT, whereas CCN increased only slightly. Nucleation particles increased in conjunction with Aitken and accumulate particles, indicating that the increase of particles relied not only on primary emissions, but also on secondary aerosol formation. At the same time, SO_4^{2-}, NO_3^-

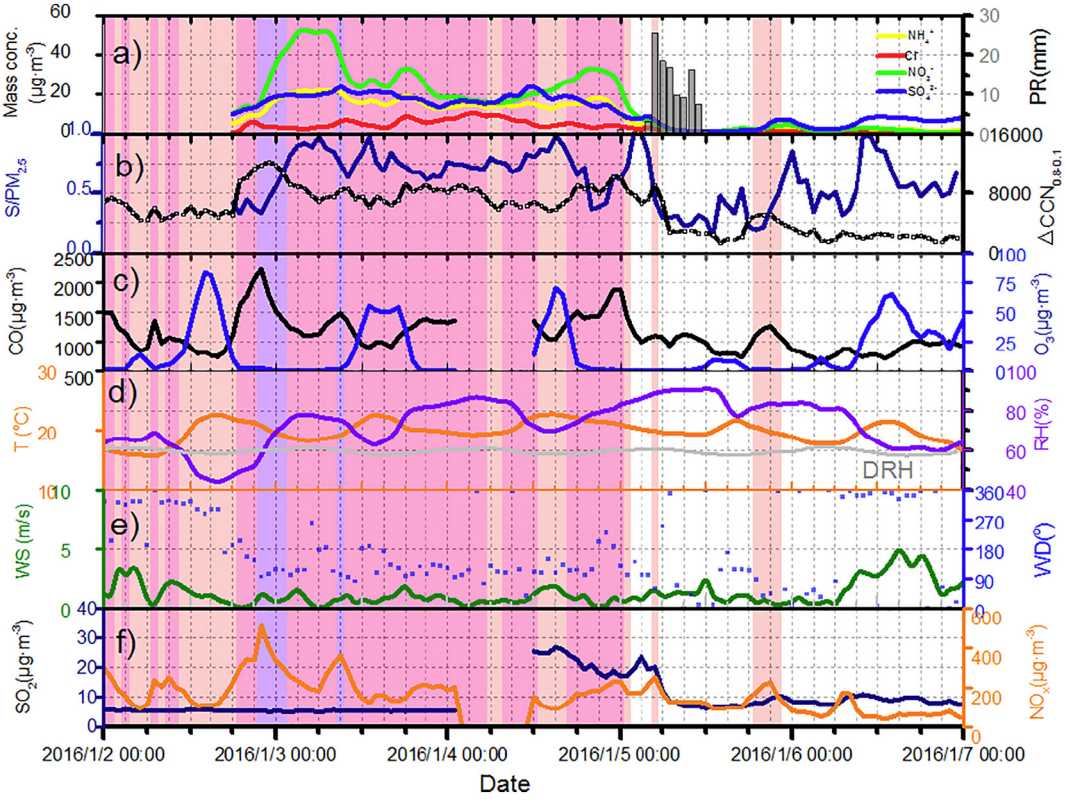

Fig. 9. Similar as Fig. 2, but for 2 to 7 January 2016. Additionally, (a) precipitation levels are displayed.

and NH_4^+ concentrations rose drastically; in particular, NO_3^- increased sharply from 16.7 μg m^{-3} to 48.3 μg m^{-3}, i.e., to a far greater extent than the other two components. To our knowledge, nitrite mainly originates from the transformation of NO and NO_2 emitted by vehicles.

3.2.2. Water-soluble chemical species in particles

The chemical species NO_3^- and NH_4^+ were more sensitive to precursor gaseous pollutants, such as CO and NO_x (Fig. 9). In addition, NO_x covaried with CO, fluctuating simultaneously and remaining at high levels at the same time. A high level of NO_X and low photochemical activity usually produce insufficient oxidants, such as OH and H_2O_2 radicals (X. Huang et al., 2014). As shown in Fig. 10, the soluble chemical compositions of particles increased following the increase in PM levels, which is similar to observations from summer. CN concentration increased with worsening pollution, but CCN/CN was not necessarily related to pollution state, especially for heavy pollution. The exact reason for this trend may be particle eruption due to emissions from motor vehicles during rush hour traffic in winter. At the same $PM_{2.5}$ level, although CO remained at high levels, SOR and NOR were low under higher RH conditions. When RH was greater than DRH, the components of particulate matter tended to become stable in the absence of strong local emissions which also should take into account of particle pH and mixing state.

The highest nitrate levels occurred several hours after minimal S/$PM_{2.5}$, whereas $\Delta CCN_{1.0-0.2}$ remained at high levels and changed constantly, indicating a huge contribution of secondary transformation to particle growth and aging. In terms of the variations in CO and NO_x over time, the burst of NO_3^- closely followed their increasing variability. Additionally, the subsequent two large peaks of nitrate changed synchronously with greater CN and $PM_{2.5}$, but lower S/$PM_{2.5}$ and relatively high $\Delta CCN_{1.0-0.2}$, probably due to constant equilibration among the high levels of chemical components under stable meteorological conditions with relatively simple exhaust pollutants. Furthermore, most particles shifting to larger sizes had heavy loadings, exceeding 20,000 cm^{-3} (Figs. 8 and S2). The growth of pre-existing particles to larger sizes during the following stages is always supported by condensation, heterogeneous reactions of chemical compounds and coagulation of particles (Wang et al., 2013).

Nevertheless, aerosol accumulation and dilution also play significant roles in particle evolution, and therefore the sources of air mass flow should be taken into account. Airflow originating in the local area contained a large amount of anthropogenic pollution on 2 to 3 January

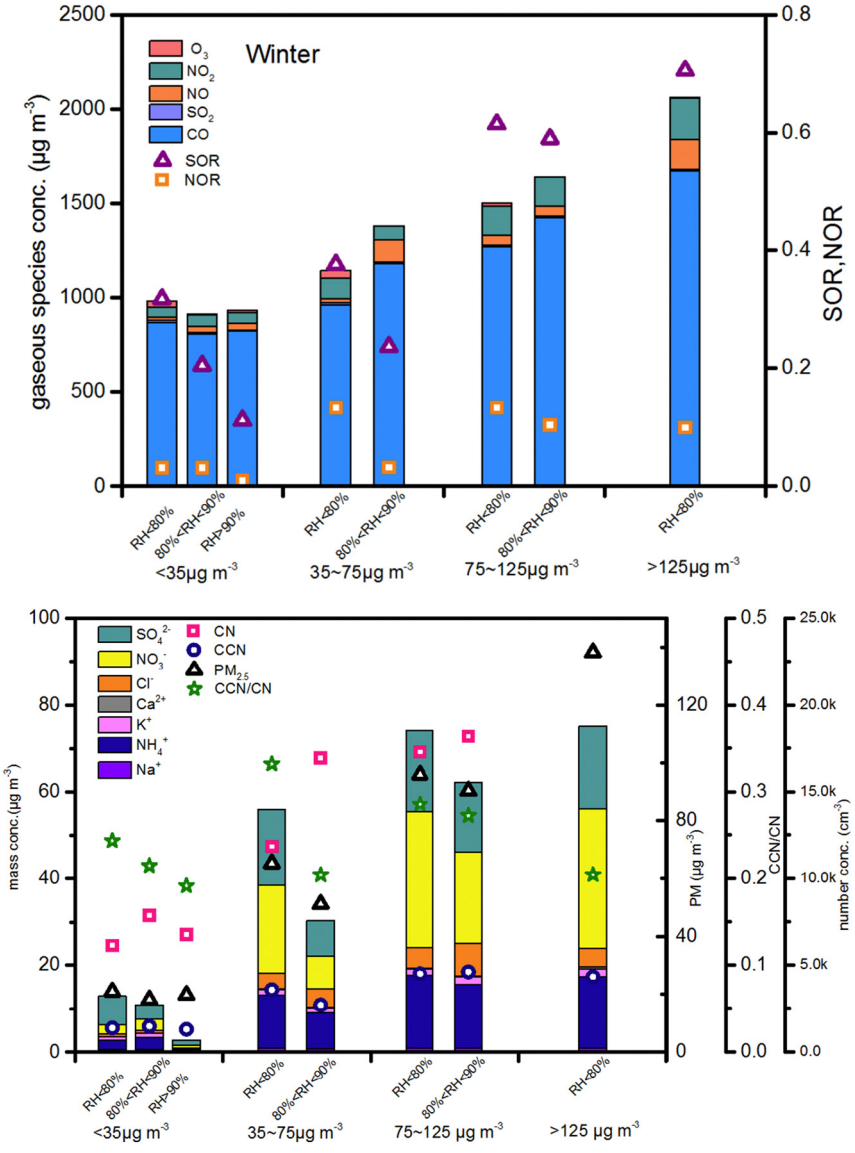

Fig. 10. Similar as Fig. 3, but for 2 to 6 January 2016.

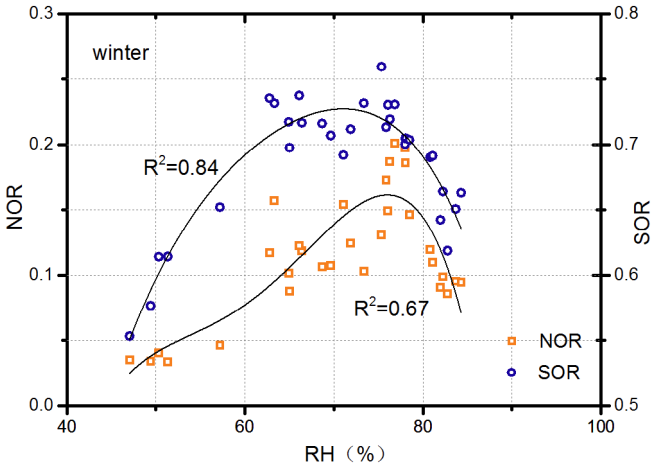

Fig. 11. Scatter plots of the transition ratios of SO_2 to SO_4^{2-} (SOR) and NO_2 to NO_3^- (NOR) vs. relative humidity (RH) during 2 to 6 January.

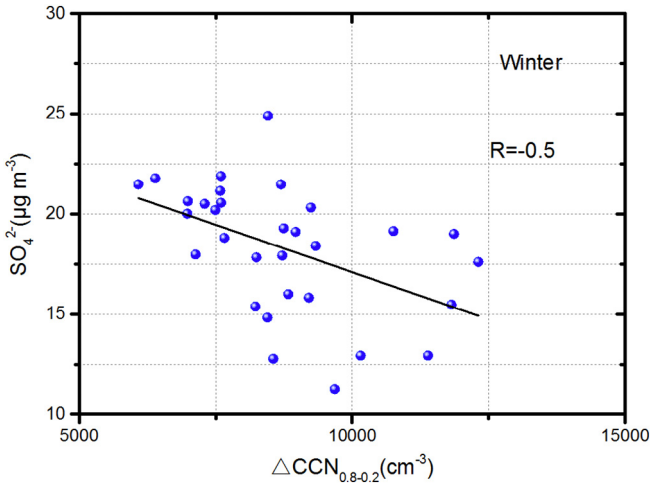

Fig. 12. Similar as Fig. 5, but for 2 to 6 January.

(Fig. S3). This large quantity of pollutants from local and regional industrial and vehicle emissions was suspending under stagnant atmospheric conditions, resulting in heavier pollution in Guangzhou.

3.2.3. Influence of pollutants on aerosol CCN activity

Fig. 11 shows the correlations of the parameters SOR and NOR with RH obtained from polynomial analysis fitting, with R^2 values (0.88 and 0.75, respectively) higher than those of lower temperature of winter. Thus, both SOR and NOR were highly influenced by RH in winter. Wang et al. (2016) reported that high humidity and low photochemical activity during hazy periods facilitate the secondary transition processes of SO_4^{2-}, NO_3^- and SOC. However, both SOR and NOR increased following the increase in RH, but then decreased when RH was >80%, emphasizing the necessity of investigating various characteristics of pollution and regional conditions thoroughly. A high amount of rainfall in January 2016 may be one contributor to the high ambient RH that was a major factor in winter haze. Similar to our results, Sun et al. (2013) found that sulfur oxidation depends directly on RH, indicating an important role of aqueous processes on sulfate formation. In addition, nitrate is more easily formed by gas-particle processing of gaseous nitric acid to aerosols under the lower T of winter (Tao et al., 2012).

Based on previous analysis, this pollution situation was caused by the rapid increase in emissions of high particulate matter concentrations containing high levels of organic compounds. To our knowledge, nucleation particles rely mainly on NPF or primary exhaust particles, while larger submicron particles are dependent on secondary particle formation and growth via gas-liquid phase changes or heterogeneous reactions (Laaksonen et al., 2005). Fig. 12 shows the negative correlation between SO_4^{2-} and $\Delta CCN_{1.0-0.2}$, indicating that lower chemical component contents in particles are primary found in small, newly formed particles that possess a large fraction of organic compounds. Under conditions of ambient RH greater than DRH, heterogeneous reaction was the dominant cause of pollution formation under high pollutant conditions in winter. The hygroscopicity parameter kappa had a positive correlation with CCN/CN (Fig. 13), implying that aerosol CCN activity obeys the usual rule whereby the fraction of activated CN concentration increases with hygroscopicity. Taking a broad view, the participation of anthropogenic pollutants in heterogeneous reactions likely acts as the main source and factor influencing winter pollution in Guangzhou.

3.3. Influence of pollutants on aerosol CCN activity during post-rain periods

Wet scavenging caused by PR can remove particles from the atmosphere, reduce pollutants and even improve air quality to some extent. After rain scouring, the atmosphere becomes very clean, and this period offers a good opportunity to study the formation and transformation of local particulate pollutants in detail. Here we investigated such conditions in winter.

Wet scavenging due to PR occurred on 5 January, starting at midnight and continuing until noon. In Fig. 8, it is apparent that accumulation mode particles were more sensitive to heavy rain scavenging (6:00–12:00 LT) than other particle modes, but responded differently during 0:00–6:00 LT under light rainfall conditions. These differing responses of particles to wet scavenging illustrated that rain can generally remove particles and may even modify the modes of particles. Compared with the large changes of $PM_{2.5}$, inorganic water-soluble chemical compositions change smoothly, and stayed at relatively low levels four several hours even after rain. The wet scavenging process and planet boundary layer (PBL) might be responsible to this pattern (Sun et al., 2011). Another possible explanation for this effect is that the continuing rise of RH may promote more ambient water vapor to mix with small particles in heterogeneous chemical reactions on the surface of atmospheric particles (Spracklen et al., 2008).

After PR ended, no immediate quick formation both for particle concentration (CN, CCN) and other particle components was observed until 18:00 LT. Accompanied by stagnant weather condition and weak photochemistry effect, the contribution of new particle formation to winter pollution can be ignored in winter. However, the increase of $S/PM_{2.5}$

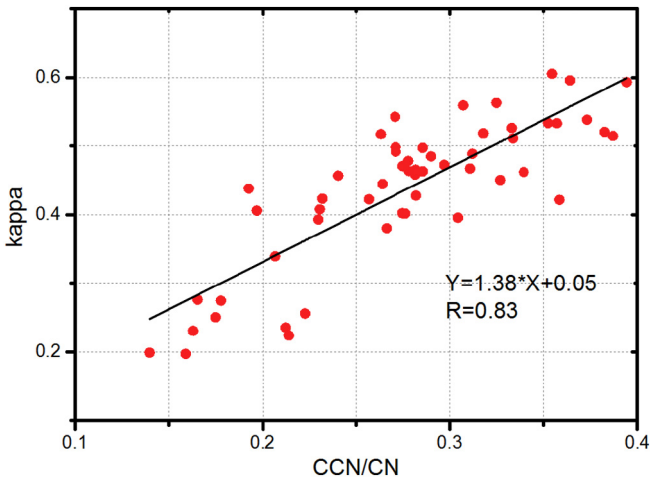

Fig. 13. Scatter plots of CCN/CN ratios vs. particle hygroscopic parameter kappa (κ) for 2 to 5 January.

displayed the change of particle compositions, implying that the particles were still under growth and aging process. The particle loading increased sharply around 20:00 LT (rush hour), when CN, CCN and $PM_{2.5}$ concentrations increased to their peaks followed by the chemical component peaks 2 h later. At the same time, CCN/CN decreased to valley value. It was apparent to see that the dominant pollution source is largely from anthropogenic emissions and large fraction of exhausted particles is hydrophobic. Moreover, the largest inorganic fraction of secondary formed particles was taken up by SO_4^{2-} instead of NO_3^-. The reason for this phenomenon may be related to the quantity of gas pollution and the ambient meteorological conditions which influenced the process of heterogeneous reactions. In winter, the atmospheric oxidation mainly relied on NO_x enhancing SO_2 oxidation by NO_2 in high ambient RH (Wang et al., 2016).

Based on this above analysis, it is apparent that the scavenging process makes a significant contribution to pollution dilution. In addition, with weak photochemical effects, the contribution of new particle formation to pollution is negligible. The effects of anthropogenic emissions are pronounced, supplying the predominant sources of particle growth and aging, and causing different transformations under different pollution conditions.

4. Conclusion

The urban pollution provides an important chance for anthropogenic pollutants to affect physical, chemical and hygroscopic properties of CCN on the ground. The characteristics of aerosol and CCN were measured for pollution cases to explore the effects of pollutants on aerosol CCN activity in the megacity Guangzhou.

Aerosol and CCN show similar paces at different pollution conditions, while aerosol CCN activity exhibits an opposite trend to the two formers. Secondary particle formation, aerosol growth and aging all play important roles in changing particle number and size, even chemical composition and mixing state to result in variation of aerosol CCN activity both in summer and winter pollution processes. Photochemical, atmospheric oxidation and heterogeneous reactions significantly impact particles in all size modes and inorganic soluble chemical compositions, and then possibly promote aerosol hygroscopicity and CCN activity. For example, photochemical reactions strongly impacted sulfur transition in summer but nitrate formation in winter. On the other hand, under strong solar radiation conditions in daytime, although inorganic chemical components increase, their proportions in particles gradually decrease probably due to the generation of organic components via photochemical reactions.

Wet scavenging can largely modify the particle modes and decrease aerosol chemical compositions. In winter, accompanied by stagnant weather condition and weak photochemistry effect, the contribution of new particle formation to pollution can be ignored. Instead, the atmospheric oxidation by anthropogenic emissions enhanced the pollution proceeding both in two seasons.

Acknowledgements

This research is supported by the National Key R&D Program of China (2017YFC1501405, 2016YFC0202000: Task 3), the National Natural Science Foundation of China (41475109, 41775129, 91637101, 21607056), and partly by the Guangdong Province Public Interest Research and Capacity Building Special Fund (2014B020216005) and the Science and Technology Commission of Shanghai Municipality (16ZR1431700).

Appendix A. Supplementary data

Supplementary data to this article can be found online at https://doi.org/10.1016/j.scitotenv.2018.06.053.

References

Alfarra, M.R., et al., 2012. The effect of photochemical ageing and initial precursor concentration on the composition and hygroscopic properties of beta-caryophyllene secondary organic aerosol. Atmos. Chem. Phys. 12, 6417–6436.
Alfarra, M.R., Good, N., Wyche, K.P., Hamilton, J.E., Monks, P.S., Lewis, A.C., McFiggans, G., 2013. Water uptake is independent of the inferred composition of secondary aerosols derived from multiple biogenic VOCs. Atmos. Chem. Phys. 13 (23), 11769–11789.
Almeida, G.P., Brito, J., Morales, C.A., et al., 2014. Measured and modelled cloud condensation nuclei (CCN) concentration in São Paulo, Brazil: the importance of aerosol size-resolved chemical composition on CCN concentration prediction. Atmos. Chem. Phys. 14 (14), 7559–7572.
Andreae, M.O., Rosenfeld, D., 2008. Aerosol-cloud-precipitation interactions. Part 1. The nature and sources of cloud-active aerosols. Earth Sci. Rev. 89, 13–41.
Arndt, J., Sciare, J., Mallet, M., et al., 2017. Sources and mixing state of summertime background aerosol in the north-western Mediterranean basin. Atmos. Chem. Phys. 17 (11), 6975–7001.
Asmi, E., Kivekäs, N., Kerminen, et al., 2011. Secondary new particle formation in Northern Finland Pallas site between the years 2000 and 2010. Atmos. Chem. Phys. 11 (24), 12959–12972.
Che, H.C., Zhang, X.Y., Wang, Y.Q., et al., 2016. Characterization and parameterization of aerosol cloud condensation nuclei activation under different pollution conditions. Sci. Rep. 6, 24497.
Cheng, Y., Zheng, G., Wei, C., et al., 2016. Reactive nitrogen chemistry in aerosol water as a source of sulfate during haze events in China. Sci. Adv. 2 (12), e1601530.
Crosbie, E., Youn, J.S., et al., 2015. On the competition among aerosol number, size and composition in predicting CCN variability: a multi-annual field study in an urbanized desert. Atmos. Chem. Phys. 15, 6943–6958.
Dai, L., Wang, H., Zhou, L., et al., 2017. Regional and local new particle formation events observed in the Yangtze River Delta region, China. J. Geophys. Res. Atmos. 122 (4), 2389–2402.
Ding, A.J., Fu, C.B., Yang, X.Q., et al., 2013. Ozone and fine particle in the western Yangtze River Delta: an overview of 1yr data at the SORPES station. Atmos. Chem. Phys. 13, 5813–5830.
Duan, J., Tao, J., Wu, Y., et al., 2017. Comparison of aerosol and cloud condensation nuclei between wet and dry seasons in Guangzhou, southern China. Sci. Total Environ. 607, 11–22.
Dusek, U., Frank, G.P., Hildebrandt, L., et al., 2006. Size matters more than chemistry for cloud-nucleating ability of aerosol particles. Science 312, 1375–1378.
Fu, H., Chen, J., 2017. Formation, features and controlling strategies of severe haze-fog pollutions in China. Sci. Total Environ. 578, 121–138.
Grivas, G., Cheristanidis, S., Chaloulakou, A., 2012. Elemental and organic carbon in the urban environment of Athens. Seasonal and diurnal variations and estimates of secondary organic carbon. Sci. Total Environ. 414, 535–545.
Gunthe, S.S., King, S.M., Rose, D., et al., 2009. Cloud condensation nuclei in pristine tropical rainforest air of Amazonia: size-resolved measurements and modeling of atmospheric aerosol composition and CCN activity. Atmos. Chem. Phys. 9, 7551–7575.
Gunthe, S.S., Rose, D., Su, H., et al., 2011. Cloud condensation nuclei (CCN) from fresh and aged air pollution in the megacity region of Beijing. Atmos. Chem. Phys. 11 (21), 11023–11039.
He, L.Y., Hu, M., Zhang, Y.H., Huang, X.F., Yao, T.T., 2008. Fine particle emissions from on-road vehicles in the Zhujiang Tunnel, China. Environ. Sci. Technol. 42 (12), 4461–4466.
Hu, G., Zhang, Y., Sun, J., Zhang, L., Shen, X., et al., 2014. Variability, formation and acidity of water-soluble ions in $PM_{2.5}$ in Beijing based on the semi-continuous observations. Atmos. Res. 145, 1–11.
Huang, R.J., Zhang, Y., Bozzetti, C., et al., 2014a. High secondary aerosol contribution to particulate pollution during haze events in China. Nature 514 (7521), 218.
Huang, X., Song, Y., Zhao, C., Li, M., Zhu, T., Zhang, Q., Zhang, X., 2014b. Pathways of sulfate enhancement by natural and anthropogenic mineral aerosols in China. J. Geophys. Res. 119, 14165–14179.
IPCC: Climate Change 2013, 2013. In: Joussaume, S., Penner, J., Tangang, F. (Eds.), The Physical Science Basis. Contribution of Working Group I to the Fifth Assessment Report of the Intergovernmental Panel on Climate Change. IPCC, Stockholm.
Kalivitis, N., Kerminen, V.M., Kouvarakis, G., et al., 2015. Atmospheric new particle formation as a source of CCN in the eastern Mediterranean marine boundary layer. Atmos. Chem. Phys. 15, 9203–9215.
Kalkavouras, P., Bossioli, E., Bezantakos, S., et al., 2017. New particle formation in the southern Aegean Sea during the Etesians: importance for CCN production and cloud droplet number. Atmos. Chem. Phys. 17 (1), 175–192.
Kerminen, V.M., Paramonov, M., Anttila, T., et al., 2012. Cloud condensation nuclei production associated with atmospheric nucleation: a synthesis based on existing literature and new results. Atmos. Chem. Phys. 12 (24), 12037–12059.
Khain, A.P., 2009. Notes on the state-of-the-art investigations of aerosol effects on precipitation: a critical review. Environ. Res. Lett. 4, 015004.
Kim, N., Park, M., Yum, S.S., et al., 2017. Hygroscopic properties of urban aerosols and their cloud condensation nuclei activities measured in Seoul during the MAPS-Seoul campaign. Atmos. Environ. 153, 217–232.
Kong, L.D., Zhao, X., Sun, Z.Y., et al., 2014. The effects of nitrate on the heterogeneous uptake of sulfur dioxide on hematite. Atmos. Chem. Phys. 14 (17), 9451–9467.
Kristensen, T.B., Müller, T., Kandler, K., et al., 2016. Properties of cloud condensation nuclei (CCN) in the trade wind marine boundary layer of the western North Atlantic. Atmos. Chem. Phys. 16 (4), 2675–2688.
Kuang, C., McMurry, P.H., McCormick, A.V., 2009. Determination of cloud condensation nuclei production from measured new particle formation events. Geophys. Res. Lett. 36, L09822.

Kuwata, M., Kondo, Y., 2008. Dependence of size-resolved CCN spectra on the mixing state of nonvolatile cores observed in Tokyo. J. Geophys. Res. Atmos. 113 (D19).
Kuwata, M., Kondo, Y., Miyazaki, Y., et al., 2008. Cloud condensation nuclei activity at Jeju Island, Korea in spring 2005. Atmos. Chem. Phys. 8, 2933–2948.
Laaksonen, A., Hamed, A., Joutsensaari, J., et al., 2005. Cloud condensation nucleus production from nucleation events at a highly polluted region. Geophys. Res. Lett. 32, L06812.
Lai, S., Zhao, Y., Ding, A., et al., 2016. Characterization of $PM_{2.5}$ and the major chemical components during a 1-year campaign in rural Guangzhou, Southern China. Atmos. Res. 167, 208–215.
Lance, S., Medina, J., Smith, J.N., Nenes, A., 2006. Mapping the operation of the DMT continuous flow CCN counter. Aerosol Sci. Technol. 40, 242–254.
Lance, S., Raatikainen, T., Onasch, T.B., et al., 2013. Aerosol mixing state, hygroscopic growth and cloud activation efficiency during MIRAGE 2006. Atmos. Chem. Phys. 13 (9), 5049–5062.
Leng, C., Zhang, Q., Tao, J., et al., 2014. Impacts of new particle formation on aerosol cloud condensation nuclei (CCN) activity in Shanghai: case study. Atmos. Chem. Phys. 14, 11353–11365.
Leng, C., Duan, J., Xu, C., et al., 2016. Insights into a historic severe haze event in Shanghai: synoptic situation, boundary layer and pollutants. Atmos. Chem. Phys. 16 (14), 9221–9234.
Liu, J., Zheng, Y., Li, Z., et al., 2011. Analysis of cloud condensation nuclei properties at a polluted site in southeastern China during the AMF-China campaign. J. Geophys. Res.-Atmos. 116 (D16).
Liu, X.G., Li, J., Qu, Y., et al., 2013. Formation and evolution mechanism of regional haze: a case study in the megacity Beijing, China. Atmos. Chem. Phys. 13, 4501–4514.
Liu, H.J., Zhao, C.S., Nekat, B., et al., 2014. Aerosol hygroscopicity derived from size-segregated chemical composition and its parameterization in the North China Plain. Atmos. Chem. Phys. 14 (5), 2525–2539.
Ma, N., Zhao, C., Tao, J., et al., 2016. Variation of CCN activity during new particle formation events in the North China Plain. Atmos. Chem. Phys. 16 (13), 8593–8607.
Mallet, M.D., Cravigan, L.T., Milic, A., et al., 2017. Composition, size and cloud condensation nuclei activity of biomass burning aerosol from northern Australian savannah fires. Atmos. Chem. Phys. 17 (5), 3605–3617.
Matsui, H., Koike, M., Kondo, Y., et al., 2011. Impact of new particle formation on the concentrations of aerosols and cloud condensation nuclei around Beijing. J. Geophys. Res.-Atmos. 116, D19.
Meng, J.W., Yeung, M.C., et al., 2014. Size-resolved cloud condensation nuclei (CCN) activity and closure analysis at the HKUST supersite in Hong Kong. Atmos. Chem. Phys. 14, 10267–10282.
Peng, J.F., Hu, M., Wang, Z.B., et al., 2014. Submicron aerosols at thirteen diversified sites in China: size distribution, new particle formation and corresponding contribution to cloud condensation nuclei production. Atmos. Chem. Phys. 14, 10249–10265.
Pierce, J.R., Adams, P.J., 2009. Uncertainty in global CCN concentrations from uncertain aerosol nucleation and primary emission rates. Atmos. Chem. Phys. 9, 1339–1356.
Qi, X.M., Ding, A.J., Nie, W., et al., 2015. Aerosol size distribution and new particle formation in the western Yangtze River Delta of China: 2 years of measurements at the SORPES station. Atmos. Chem. Phys. 15, 12445–12464.
Rogers, R.R., Yau, M.K., 1989. A Short Course in Cloud Physics. 3rd ed. Pergamon Press, Oxford, New York, USA (293 pp.).
Rose, D., Gunthe, S.S., Mikhailov, E., et al., 2008. Calibration and measurement uncertainties of a continuous-flow cloud condensation nuclei counter (DMT-CCNC): CCN activation of ammonium sulfate and sodium chloride aerosol particles in theory and experiment. Atmos. Chem. Phys. 8 (5), 1153–1179.
Rose, D., Nowak, A., Achtert, P., et al., 2010. Cloud condensation nuclei in polluted air and biomass burning smoke near the mega-city Guangzhou, China-part 1: size-resolved measurements and implications for the modeling of aerosol particle hygroscopicity and CCN activity. Atmos. Chem. Phys. 10 (7), 3365–3383.
Rosenfeld, D., Lohmann, U., Raga, G.B., et al., 2008. Flood or drought: how do aerosols affect precipitations? Science 321:1309–1313. https://doi.org/10.1126/science.1160606.
Seinfeld, J.H., Pandis, S.N., 2006. Atmospheric Chemistry and Physics: From Air Pollution to Climate Change. 2nd edn. John Wiley & Sons, New York, USA (57–58 and 381–383).
Sihto, S.L., Mikkilä, J., Vanhanen, J., et al., 2011. Seasonal variation of CCN concentrations and aerosol activation properties in boreal forest. Atmos. Chem. Phys. 11, 13269–13285.
Spracklen, D.V., Carslaw, K.S., Kulmala, M., et al., 2008. Contribution of particle formation to global cloud condensation nuclei concentrations. Geophys. Res. Lett. 35 (6).
Sun, Y.L., Zhang, Q., Schwab, J.J., et al., 2011. A case study of aerosol processing and evolution in summer in New York City. Atmos. Chem. Phys. 11 (24), 12737–12750.
Sun, Y.L., Wang, Z.F., Fu, P.Q., et al., 2013. Aerosol composition, sources and processes during wintertime in Beijing, China. Atmos. Chem. Phys. 13, 4577–4592.
Sun, Y.L., Zhang, Q., Wang, Z., et al., 2014. Investigation of the sources and evolution processes of severe haze pollution in Beijing in Juanuary 2013. J. Geophys. Res.-Atmos. 119, 4380–4398.
Svensmark, H., Enghoff, M.B., Shaviv, N.J., Svensmark, J., 2017. Increased ionization supports growth of aerosols into cloud condensation nuclei. Nat. Commun. 8 (1), 2199.
Tao, J., Shen, Z.X., Zhu, C.S., et al., 2012. Seasonal variations and chemical characteristics of sub-micrometer particles (PM_1) in Guangzhou, China. Atmos. Res. 118, 222–231.
Tao, J., Zhang, I.M., Cao, J.J., et al., 2017. Source apportionment of $PM_{2.5}$ at urban and suburban areas of the Pearl River Delta region, south China - with emphasis on ship emissions. Sci. Total Environ. 574, 1559–1570.
Tian, M., Wang, H., Chen, Y., et al., 2016. Characteristics of aerosol pollution during heavy haze events in Suzhou, China. Atmos. Chem. Phys. 16 (11), 7357–7371.
Vogel, A.L., Schneider, J., Müller-Tautges, C., et al., 2016. Aerosol chemistry resolved by mass spectrometry: linking field measurements of cloud condensation nuclei activity to organic aerosol composition. Environ. Sci. Technol. 50 (20), 10823–10832.
Wang, J., Cubison, M.J., Aiken, A.C., Jimenez, J.L., Collins, D.R., 2010. The importance of aerosol mixing state and size-resolved composition on CCN concentration and the variation of the importance with atmospheric aging of aerosols. Atmos. Chem. Phys. 10, 7267–7283.
Wang, Z., Wang, T., Guo, J., et al., 2012. Formation of secondary organic carbon and cloud impact on carbonaceous aerosols at Mount Tai, North China. Atmos. Environ. 46, 516–527.
Wang, Y., Zhang, Q.Q., He, K., Zhang, Q., Chai, L., 2013. Sulfate-nitrate-ammonium aerosols over China: response to 2000–2015 emission changes of sulfur dioxide, nitrogen oxides, and ammonia. Atmos. Chem. Phys. 13, 263–265.
Wang, Y.H., Liu, Z.R., Zhang, J.K., et al., 2015. Aerosol physicochemical properties and implications for visibility during an intense haze episode during winter in Beijing. Atmos. Chem. Phys. 15, 3205–3215.
Wang, G.H., Zhang, R.Y., Gomez, M.E., et al., 2016. Persistent sulfate formation from London fog to Chinese haze. Proc. Natl. Acad. Sci. 113 (48), 13630–13635.
Wex, H., McFiggans, G., Henning, S., Stratmann, F., 2010. Influence of the external mixing state of atmospheric aerosol on derived CCN number concentrations. Geophys. Res. Lett. 37, L10805.
Wiedensohler, A., Cheng, Y.F., Nowak, A., et al., 2009. Rapid aerosol particle growth and increase of cloud condensation nucleus activity by secondary aerosol formation and condensation: a case study for regional air pollution in northeastern China. J. Geophys. Res.-Atmos. 114, D00G08.
Wildt, J., et al., 2014. Suppression of new particle formation from monoterpene by NOx. Atmos. Chem. Phys. 14, 2789–2804.
Wu, Z.J., Poulain, L., Birmili, W., et al., 2015. Some insights into the condensing vapors driving new particle growth to CCN sizes on the basis of hygroscopicity measurements. Atmos. Chem. Phys. 15, 13071–13083.
Xu, H., Cao, J., Chow, J.C., et al., 2016. Inter-annual variability of wintertime $PM_{2.5}$ chemical composition in Xi'an, China: evidences of changing source emissions. Sci. Total Environ. 545, 546–555.
Yuan, C., Ma, Y., Diao, Y., et al., 2017. CCN activity of secondary aerosols from terpene ozonolysis under atmospheric relevant conditions. J. Geophys. Res. Atmos. 122 (8), 4654–4669.
Yue, D.L., Hu, M., Zhang, R.Y., et al., 2010. The roles of sulfuric acid in new particle formation and growth in the mega-city of Beijing. Atmos. Chem. Phys. 10 (10), 4953–4960.
Yum, S.S., Hudson, J.G., Song, K.Y., et al., 2005. Springtime cloud condensation nuclei concentrations on the west coast of Korea. Geophys. Res. Lett. 32 (9).
Zhao, C., Tie, X., Brasseur, G., et al., 2006. Aircraft measurements of cloud droplet spectral dispersion and implications for indirect aerosol radiative forcing. Geophys. Res. Lett. 33, L16809.
Zhao, D.F., Buchholz, A., Kortner, B., et al., 2015. Size-dependent hygroscopicity parameter (κ) and chemical composition of secondary organic cloud condensation nuclei. Geophys. Res. Lett. 42 (24).
Zheng, J.Y., Yin, S.S., Kang, D.W., et al., 2012. Development and uncertainty analysis of a high-resolution NH_3 emissions inventory and its implications with precipitation over the Pearl River Delta region, China. Atmos. Chem. Phys. 12 (15), 7041–7058.